HHS Public Access

Author manuscript

Oncogene. Author manuscript; available in PMC 2015 September 26.

Published in final edited form as:

Oncogene. 2015 March 26; 34(13): 1619–1628. doi:10.1038/onc.2014.98.

Two mature products of *MIR-491* coordinate to suppress key cancer hallmarks in glioblastoma

Xia Li[#1,6], **Yuexin Liu**[#1], **Kirsi J. Granberg**[1,7,8], **Qinhao Wang**[6], **Lynette M. Moore**[1], **Ping Ji**[1], **Joy Gumin**[2], **Erik P. Sulman**[3], **George A. Calin**[4,5], **Hannu Haapasalo**[8], **Matti Nykter**[7,9], **Ilya Shmulevich**[10], **Gregory N. Fuller**[1], **Frederick F. Lang**[2], and **Wei Zhang**[1,5,*]

[1]Department of Pathology, The University of Texas MD Anderson Cancer Center, Houston, Texas, USA [2]Department of Neurosurgery, The University of Texas MD Anderson Cancer Center, Houston, Texas, USA [3]Department of Radiation Oncology, The University of Texas MD Anderson Cancer Center, Houston, Texas, USA [4]Department of Experimental Therapeutics, The University of Texas MD Anderson Cancer Center, Houston, Texas, USA [5]Department of Non-coding RNA center, The University of Texas MD Anderson Cancer Center, Houston, Texas, USA [6]Department of Biochemistry and Molecular Biology, State Key Laboratory of Cancer Biology, The Fourth Military Medical University, Xi'an, China [7]Department of Signal Processing, Tampere University of Technology, Tampere, Finland [8]Department of Pathology, Fimlab Laboratories and University of Tampere, Tampere, Finland [9]Institute of Biomedical Technology, University of Tampere, Tampere, Finland [10]Institute for Systems Biology, Seattle, Washington, USA

[#] These authors contributed equally to this work.

Abstract

MIR-491 is commonly co-deleted with its adjacent *CDKN2A* on chromosome 9p21.3 in glioblastoma (GBM). However, it is not known whether deletion of *MIR-491* is only a passenger event or plays an important role. Small-RNA sequencing of samples from GBM patients demonstrated that both mature products of *MIR-491* (miR-491-5p and -3p) are downregulated in tumors compared to normal brain. The integration of GBM data from The Cancer Genome Atlas (TCGA), miRNA target prediction and reporter assays showed that miR-491-5p directly targets *EGFR*, *CDK6*, and *Bcl-xL*, whereas miR-491-3p targets *IGFBP2* and *CDK6*. Functionally, miR-491-3p inhibited glioma cell invasion; overexpression of both miR-491-5p and -3p inhibited proliferation of glioma cell lines and impaired the propagation of glioma stem cells (GSCs), thereby prolonging survival of xenograft mice. Moreover, knockdown of miR-491-5p in primary *Ink4a-Arf*-null mouse glial progenitor cells exacerbated cell proliferation and invasion. Therefore, *MIR-491* is a tumor suppressor gene that, by utilizing both mature forms, coordinately controls key cancer hallmarks: proliferation, invasion, and stem cell propagation.

[*]Correspondence: Wei Zhang, PhD, Department of Pathology, Unit 85, The University of Texas MD Anderson Cancer Center, 1515 Holcombe Blvd., Houston, TX 77030; telephone: 713-745-1103; fax: 713-792-5549; wzhang@mdanderson.org..

CONFLICT OF INTEREST

The authors declare no conflict of interest.

Keywords

miR-491; CDKN2A; glioma stem cell; GBM; IGFBP2; CDK6; EGFR

INTRODUCTION

Genome instability is the prevalent cancer characteristic, having a major role in enabling the development of different cancer hallmarks[1]. It is commonly manifested by the deletion of chromosomal regions[2], leading often to inactivation of tumor suppressor genes. The best recognized deleted tumor suppressor genes include *PTEN* (10q23)[2], *RB1* (13q14)[3], *TP53* (17p13)[3], and *CDKN2A* (9p21.3, encoding $p16^{INK4a}$ and $p14^{ARF}$)[4-7 4-7]. However, whether the concurrently deleted genes within these regions play important roles or only serve as passenger events in cancer pathogenesis is not well established.

MicroRNAs (miRNAs) are ~21-nt single-stranded small RNAs that modulate gene expression by targeting the 3′-untranslated region (3′-UTR) of mRNAs and promoting RNA degradation and/or inhibiting its translation[8]. MiRNAs play important roles in various cellular processes by simultaneously regulating the expression levels of hundreds of genes[8]. They have also been shown to function as key players in cancer by regulating the expression of various oncogenes and tumor suppressors[9]. By analyzing The Cancer Genome Atlas (TCGA) data from different cancer types, we found that a microRNA-encoding gene, *MIR-491*, is commonly deleted together with *CDKN2A* in many cancers, including glioblastoma multiforme (GBM). *MIR-491* produces two mature miRNAs, miR-491-5p and miR-491-3p. Although miR-491-5p has been shown to induce apoptosis of colon cancer cells by targeting Bcl-xL[10] and to inhibit migration of glioma cells by targeting MMP-9[11], the biological function of miR-491-3p in GBM is not characterized and most importantly, systematic investigation of coordinate role of the two mature miRNAs generated from the same precursor in GBM pathogenesis has been poorly studied.

In this study, we sought to investigate whether *MIR-491* functions as a tumor suppressor gene in GBM. We found that expressions of both miR-491-3p and miR-491-5p were downregulated in GBM compared with normal brain. Integrated analysis of 388 GBM samples from TCGA coupled with miRNA-mRNA prediction tools identified several key oncogenes, including *IGFBP2*, *CDK6*, *EGFR*, and *Bcl-xL*, as targets of miR-491-5p and -3p. We confirmed that *IGFBP2* and *CDK6* can be regulated directly by miR-491-3p, while *EGFR*, *CDK6*, and *Bcl-xL* can be targeted by miR-491-5p. Forced expression of miR-491-3p inhibited glioma cell invasion by regulating *IGFBP2*, while global restoration of miR-491-5p and miR-491-3p restricted glioma growth and GSC propagation by coordinately regulating *EGFR*, *CDK6*, and *IGFBP2*, consequently prolonging the survival of xenograft mice. We also showed that knockdown of miR-491-5p in primary *Ink4a-Arf*-null mouse glial progenitors could further promote cell proliferation and invasion. Our results suggest that both miR-491-5p and -3p functions as key tumor suppressors by coordinately suppressing several important oncogenes in GBM.

RESULTS

miR-491-5p and -3p expression are downregulated in GBM and inversely correlated with expression of IGFBP2, EGFR, CDK6, and Bcl-xL

Human *MIR-491* is approximately 1.25 Mb distal to the *CDKN2A* gene located on chromosome 9p21.3, which is frequently deleted in a variety of cancers, including GBM (Figure 1a and b). *MIR-491* typically exhibits a similar copy alteration pattern as *CDKN2A*, a well-recognized tumor suppressor (Figure 1b). The miR-491 stem-loop produces two mature forms, miR-491-5p (major) and miR-491-3p (minor) (Figure S1A). TCGA genome-wide SNP array data from 388 GBM patients showed that genomic local deletion of *MIR-491* leads to a significant decrease in expression of miR-491-5p ($P < 0.0001$, Figure 1c), the only form for which expression values are available due to technology limitations (Agilent 8×15K Human miRNA-specific microarray). By analyzing the whole-transcriptome and small-RNA deep-sequencing data from pooled GBM and normal brain samples[12, 13], we found that both miR-491-5p and miR491-3p were present and their expression levels (read numbers) were markedly higher in the normal brain than in GBM (Figure 1f).

Because these two mature forms are derived from the same precursor, we speculated that their expression levels are correlated with each other. This is supported by TCGA endometrial and breast cancer data that have the expression data available for both mature forms (Figure 1d). Therefore, we used miR-491-5p GBM expression data from TCGA to represent both miR-491-5p and miR-491-3p expression levels and coupled this with miRNA-mRNA target predictions from Targetscan to identify the candidate targets of miR-491-5p and -3p. 681 genes were identified to be significantly and inversely correlated with miR-491-5p ($P < 0.05$), among which 211 genes are predicted targets of miR-491-3p and 526 genes are predicted targets of miR-491-5p; 56 genes are predicted to be targeted by both (Figure S1b). *IGFBP2*, a predicted target of miR-491-3p, and *CDK6*, a predicted target of both miR-491-3p and -5p, are among the genes that exhibit the greatest statistical significance of negative correlation with miR-491 expression (Figure S1b). Details of these putative targets and of their associations with the two miR-491 mature forms are summarized in Supplemental Table S1.

Pathway analysis of these putative targets showed that the two mature forms of miR-491 differentially regulate multiple signaling pathways associated with different cancer hallmarks (Figure 1e). In particular, PTEN and apoptosis signaling pathways, which involve the *EGFR* and *BCL2L1* (also known as *Bcl-xL*) genes, are significantly enriched (Fisher's exact test) in the miR-491-5p targets, while ILK and glioma signaling pathways, involving the *IGFBP2* and *CDK6* genes, are significantly enriched in the miR-491-3p targets (Figure 1e). Indeed, our whole-transcriptome sequencing data (performed in parallel to the miRNA deep-sequencing data) showed that the normalized RPKM (Reads Per Kilobase of exon model per Million mapped reads) values of *IGFBP2*, *EGFR*, *CDK6*, and *Bcl-xL* were higher in GBM samples than in normal brain (Figure 1g), as expected. We therefore hypothesized that the loss of miR-491 may contribute to upregulation of these oncogenes, with significant effects on tumor progression.

miR-491-5p and/or miR-491-3p directly target *IGFBP2, EGFR, CDK6*, and *Bcl-xL* and regulate GBM cell proliferation

According to Targetscan prediction, the binding sites for miR-491-5p are present on the 3′-UTRs of *EGFR*, *Bcl-xL*, and *CDK6*, whereas those of miR-491-3p are present on the 3′-UTRs of *IGFBP2* and *CDK6*. We transfected U251 glioma cells (expressing all of these genes) with mimics of these two miRNAs, individually or together, and found that IGFBP2 protein was downregulated by miR-491-3p, but not by -5p; EGFR and Bcl-xL were downregulated by miR-491-5p, but not by -3p; and CDK6 was downregulated by both (Figure 2a). Reporter assays in which the 3′-UTRs of these oncogenes (either containing the predicted binding sites or not) were fused downstream of luciferase further confirmed that the binding sites within *EGFR* (for miR-491-5p), *IGFBP2* (for miR-491-3p) and *CDK6* F1 (for both), but not *CDK6* F3 (for miR-491-3p) are functionally relevant (Figure S2). The 3′-UTR of *Bcl-xL* has been shown to be a direct target of miR-491-5p[10]. Together, these data indicate that miR-491-5p regulates *EGFR*, *CDK6*, and *Bcl-xL*, while miR-491-3p regulates *IGFBP2* and *CDK6* by directly targeting the corresponding 3′-UTR.

Because both miR-491-5p and miR-491-3p are transcribed concomitantly in most cells, we investigated the consequence of overall miR-491 restoration by transfecting miR-491-5p and miR-491-3p together (referred to as miR-491 hereafter) into U251 and T98G GBM cell lines, in which p16 is inactivated due to *CDKN2A* deletion[14, 15] and miR-491-5p and -3p were downregulated compared with the normal brain tissues according to the q-PCR results (Figure S3). It was shown that miR-491 significantly suppressed the growth of U251 and T98G cells, measured by MTT assay (Figure 2b) and anchorage-independent soft agar colony formation assay (Figure 2c). Furthermore, miR-491 overexpression dramatically decreased the proportion of proliferating cells when measured with BrdU incorporation assay (Figure 2d), whereas miR-491 had no significant effect on cell apoptosis (Figure S4). Thus, miR-491 directly regulates *IGFBP2*, *EGFR*, *CDK6*, and *Bcl-xL* expression and represses glioma cell proliferation.

miR-491-3p inhibits GBM cell invasion by regulating IGFBP2

As a mature form of microRNA, the function of miR-491-3p is poorly characterized and we for the first time show that miR-491-3p regulates *IGFBP2*. To evaluate this regulatory relationship *in vivo*, we performed immunohistochemical staining and *in situ* hybridization analysis measuring IGFBP2 and miR-491-3p, respectively, on a tissue microarray (TMA) representing 146 brain tumor cases (106 GBMs, 37 lower grade astrocytomas, 3 oligoastrocytomas). We observed a significant negative correlation between IGFBP2 protein level and miR-491-3p level (Figure 3a and b), underscoring the biologic relevance of such regulation.

Since IGFBP2 has been shown to be an important regulator of cell migration and invasion in different types of cancer[16-18], we examined whether miR-491-3p is involved in cell invasion. Upon transfection, miR-491-3p markedly inhibited invasion of both U251 and T98G cells (Figure 3c and d, with representative photographs shown in Figure S5) as efficiently as knockdown of *IGFBP2* via siRNA. We further examined whether IGFBP2 is a key contributor for miR-491-3p's function by performing a rescue experiment. The stable

U251 cells overexpressing either GFP (U251-GFP) or IGFBP2-EGFP (U251-IGFBP2) were established and transfected with miR-491-3p mimics. In U251-GFP, ectopic expression of miR-491-3p resulted in obvious IGFBP2 downregulation (Figure 3e, lower panel) and 50% less cell invasion than control cells (Figure 3e, upper panel). In U251-IGFBP2, miR-491-3p suppressed the endogenous IGFBP2, but not exogenous IGFBP2-EGFP, whose transcript does not contain the 3′-UTR of *IGFBP2* (Figure 3e). Overexpression of IGFBP2-EGFP increased cell invasion by 20% compared with that of U251-GFP (Figure 3e), which is consistent with previously published findings[19]. miR-491-3p decreased cell invasion by only 30% in U251-IGFBP2 cells compared to 50% in U251-GFP cells (Figure 3e), suggesting that overexpression of IGFBP2 can partly reverse the inhibitory effect of miR-491-3p on cell invasion. These results indicate that miR-491-3p inhibits cell invasion at least partially through downregulation of IGFBP2. Taken together with the previous study showing that miR-491-5p targets MMP-9 and inhibits glioma cell invasion[11], it can be concluded that both mature forms of miR-491 are suppressors of glioma invasiveness.

miR-491 impairs GSC propagation *in vitro* and *in vivo*

Increasing evidence indicates that glioma stem-like cells (GSC) are the driving force for progression and recurrence of aggressive gliomas[20]. Since IGFBP2 and EGFR have been shown to play important roles in GSC propagation or maintenance[21-23], we examined how miR-491 affects GSC cells by using two patient-derived GSC lines, GSC 11 and GSC 6-27, which grow as neurospheres in serum-free medium supplemented with EGF and bFGF[24, 25]. Both GSC 11 and GSC 6-27 are deleted for CDKN2A, as determined by Oncoscan copy number analysis. The multilineage differentiation potential of the GSCs was confirmed through examination of differentiation markers upon induction with retinoic acid (RA) or forskolin (FSK) (Figure S6). Based on the results of q-PCR, the expression levels of miR-491-5p and miR-491-3p were downregulated compared with the normal brain control (Figure S3). Thus, we transfected miR-491-5p and miR-491-3p together into GSC 11 or GSC 6-27 and then examined the resultant phenotypes. Overexpression of miR-491 significantly inhibited growth of GSCs, as indicated by significant reductions in sphere size and number (Figure 4a and S7a). Furthermore, miR-491 impaired the self-renewal ability of these neurospheres, which were demonstrated by a significant decrease of secondary and tertiary sphere formation upon serial dilutions (Figure 4b and S7b). Such effects were accompanied by inhibition of cell proliferation (Figure 4c and S7c) and induction of apoptosis (Figure 4d and S7d), which was also reflected as PARP cleavage (Figure 4f and S7f). The downregulation of IGFBP2, EGFR, CDK6, and Bcl-xL caused by miR-491 in these experiments was confirmed by Western blot analysis (Figure 4e and S7e). Phosphorylated AKT, a known downstream signal for both IGFBP2[26] and EGFR[27], was markedly reduced by miR-491 (Figure 4f and S7f). Furthermore, exogenous miR-491 led to considerable decreases in the levels of Sox2 and Nestin, both known stem/progenitor cell markers, in GSC 11 and GSC 6-27 cells, respectively (Figure 4f and S7f). This is consistent with the published finding that *IGFBP2* knockdown leads to decreases in Nestin and Sox2[21]. Finally, miR-491 increased expression of astrocytic differentiation marker GFAP in both GSCs (Figure 4f and S7f). Collectively, these data indicate that miR-491 controls the propagation of GSCs by regulating their proliferation, apoptosis, and differentiation.

We then sought to determine whether the effects of miR-491 on GSCs are mediated by their targets, *IGFBP2*, *CDK6*, *EGFR*, and *Bcl-xL*. To this end, we first observed the effect of knockdown of each of these genes on cell behavior. As shown, the knockdown efficiencies of siRNA or esiRNA were confirmed by Western blot (Figure S8a and b); knockdown of any of these genes caused significant inhibition of neurosphere formation by both GSC 11 and GSC 6-27 (Figure S8c and d), as evinced by reductions in both sphere number and size. BrdU incorporation assay and apoptosis assay showed that knockdown of IGFBP2, CDK6, or EGFR significantly inhibited GSC proliferation (Figure S8e), whereas knockdown of Bcl-xL induced a moderate apoptosis in both GSCs, with statistical significance in GSC 11 (Figure S8f). Further, for rescue experiments, we overexpressed IGFBP2, CDK6, EGFR, or Bcl-xL via expression vectors that lacked the respective 3′-UTR region and thus could not be inhibited by miR-491 (Figure 4g), and then examined their effects on miR-491's function in GSC 11. This forced expression of IGFBP2, CDK6, or EGFR, but not Bcl-xL, rescued inhibition of neurosphere formation by miR-491 (Figure 4h).

Finally, we examined whether miR-491 inhibits GBM tumor growth and affects host survival *in vivo*. GSC 11 cells were transfected with control mimics, miR-491-5p and -3p together, or left untreated. Twenty-four hours later, 1×10^5 cells were orthotopically transplanted into the brain of immunocompromised mice (10 mice/group). We found that the mice implanted with untreated GSC 11 or cells transfected with the control mimics died significantly earlier (within 70-86 days of implantation) than mice implanted with miR-491–transfected cells (90-105 days) ($P < 0.0001$, log-rank test) (Figure 4i). The difference in survival observed between the group implanted with untreated cells and the group implanted with controls was not significant.

Knockdown of miR-491-5p enhances proliferation and invasion of Ink4a-Arf-null mouse glial progenitors

Because of its location being adjacent to *CDKN2A* (encoding $p16^{INK4a}$) on chr9p21.3, loss of *MIR-491* commonly occurs concurrently with loss of *CDKN2A* in human GBM (Figure 1a and b). This raises a possibility that the strong impact of $p16^{INK4A}$ loss on tumorigenesis may mask the effect of *MIR-491* loss. Therefore, we determined whether knockdown of miR-491 is still impactful in the context of *CDKN2A* deletion. The binding sites for miR-491-5p but not miR-491-3p are evolutionarily conserved between human and mouse for the 3′-UTRs of *CDK6*, *EGFR*, and *Bcl-xL* and the regulatory role of miR-491-5p in these mouse genes was confirmed by Western blot (Figure S9). We thus examined the consequence of miR-491-5p knockdown in primary murine *Ink4a-Arf*-null glial progenitor cells. Western blot showed that transfection of miR-491-5p hairpin inhibitors reduced the levels of miR-491-5p by more than 50% (Figure 5a) and consequently increased the levels of mouse CDK6, EGFR, and Bcl-xL (Figure 5b). Consistent with this, miR-491-5p knockdown significantly increased the cell viability of *Ink4a-Arf*-null glial progenitor cells (Figure 5c), promoted cell proliferation (Figure 5d), and enhanced cell invasion (Figure 5e). Collectively, these data support the notion that loss of *MIR-491* is a critical genetic event and not merely a passenger concomitant to *CDKN2A* loss in GBM with 9p21.3 deletion.

DISCUSSION

GBM is one of the most lethal cancers and novel therapeutic interventions are urgently needed[28]. Extensive genetic and molecular studies, especially comprehensive profiling studies in TCGA, have characterized GBM-related oncogenes (e.g., *EGFR*, *PDGFRA*, *CDK6*) and tumor suppressor genes (e.g., *PTEN*, *CDKN2A*, *Arf*, *TP53*, *NF1*)[29, 30]. Gene copy number changes and mutations account for only a fraction of these alterations. Further, even for one of the most druggable events, *EGFR* amplification and overexpression, targeting *EGFR* alone has shown minimal therapeutic outcome in GBM patients[31, 32]. It is the consensus in the field that multiple pathways need to be targeted preferentially via a converging regulator. The most significant discoveries from this study are the identification and characterization of *MIR-491* as a key inactivated tumor-suppressing non–protein-coding gene. Most importantly, it can integrate the regulation of multiple GBM hallmarks by directly targeting a number of oncogenes that are known to be important for GBM.

Although *MIR-491* is located in a region (9p21.3) that is most recognizable for GBMs because of its frequent deletion, the importance of this miRNA has not been fully recognized. One possible reason is that *MIR-491* is overshadowed by its better-known neighbor, *CDKN2A* (encoding $p16^{INK4a}$ and $p14^{ARF}$), in the same chromosomal region. Indeed, although *Ink4a-Arf* null mouse models develop various spontaneous tumors at an early age and the glial cells of these mice are more vulnerable to PDGFB induced high-grade glioma, glioma is not among the spontaneous tumor types that develop in these mice[33]. This may be a hint that *CDKN2A* deletion itself is not sufficient for glioma development and other co-occurring oncogenic events within this locus are also needed, which await further in-depth investigation.

Indeed, our previous studies showed that $p16^{INKA}$ downregulation co-occurs with IGFBP2 overexpression[33]. *IGFBP2* is a recently recognized oncogene in glioma[26], promoting invasion[19, 34], angiogenesis[35], and expansion of stem cells[21]. But the mechanism for the frequent IGFBP2 overexpression in GBM has been elusive. In contrast to *EGFR* and *PDGFRA*, *IGFBP2* copy number in GBM is largely neutral (Figure S10). In this study, we determined that decreased expression of miR-491-3p due to genomic deletion is a key mechanism for elevated IGFBP2 expression via the target site on *IGFBP2* 3′-UTR. Moreover, we show that miR-491-3p is not only present in GBM, endometrial cancer, and breast cancer, but also is functional in glioma cell lines and GSC. Through regulation of *IGFBP2*, miR-491-3p is involved in regulation of glioma cell invasion and GSC propagation, both driving forces for GBM recurrence. Notably, either complete 9p21.3 loss or IGFBP2 overexpression was associated with poor prognosis of GBM[36, 37]. Our current study clearly reveals the molecular mechanism underlying these two prognostic events.

The glioma cell lines we tested were all *CDKN2A* deleted and show significant downregulation of miR-491 expression (Figure S3). Restoration of miR-491 in these cell lines resulted in inhibition in cell malignant behavior. Conversely, knockdown of miR-491-5p in the murine astrocytes (intact *MIR-491* in the context of *CDKN2A* knockout), promoted cell growth and invasion. These data indicated that *MIR-491* function as a tumor suppressor gene even with the molecular background of CDKN2A deletion.. Interestingly,

KIAA1797/FOCAD[38], which is the host gene of *MIR-491*, was recently reported to possess tumor suppressive activities in glioma. Spatial proximity of *MIR-491* with these well-recognized tumor suppressor genes implied its tumor suppressive role in GBM. Moreover, the relationship of these tumor suppressor genes appear to be interesting and certainly deserves a systematic investigation in the future.

Our investigation revealed that *MIR-491* is a master tumor suppressor gene that utilizes both mature forms to control the key hallmarks of GBM: uncontrolled cell proliferation, invasion, and stem cell propagation. Restoration of overall miR-491 blocked the growth of both GBM cell lines and patient-derived GSCs, with decreased expression of IGFBP2, CDK6, and EGFR contributing to miR-491's function in GSCs. Although IGFBP2[21] and EGFR[23, 27, 39, 40] have been established to play important roles in GSC maintenance and propagation, here we showed for the first time that CDK6, another important proto-oncogene in GBM, is also implicated in regulation of GSC behavior. This is supported by the study showing that Cdk6 deficiency prevents the expansion of neuronally committed precursors [41]. Our study and others'[42] also showed that Bcl-xL is involved in GSC apoptosis, but its overexpression does not completely abrogate the function of miR-491, given that the regulation of other targets by miR-491 is sufficient to inhibit GSC propagation. Because GSCs are believed to be responsible for recurrence of GBM after surgery and chemotherapy, we propose that miR-491-5p and -3p, by acting as key GSC regulators, may provide a new agent for GBM treatment.

miRNAs are an attractive class of therapeutic tools because of their stability and small size and several miRNAs have been shown to suppress GSCs[43-46]. Mesenchymal stem cells[47-49] and nanoparticle-mediated delivery approaches[50] are being tested actively. In this study, we tried lentiviral miR-491 to infect GSCs but we were unable to establish stable clones because of the inhibitory role of miR-491. Therefore, we performed *in vivo* experiments by transfecting GSC 11 cells with miR-491 mimics twenty-four hours before injecting them into the brains of mice. Our results show that the inhibitory role of transfected miR-491 mimics is sufficient to slow down tumor growth *in vivo* and prolong the host survival. With improvement of delivery technologies, miR-491 may emerge as a highly attractive therapeutic tool that simultaneously puts a brake on multiple oncogenic pathways in both GSCs and non-GSCs.

In summary, we propose that genomic deletion of 9p21.3 leads to concurrent loss of two key tumor suppressors: *MIR-491* and *CDKN2A*. *MIR-491* produces two mature forms, miR-491-5p and miR-491-3p, which suppress glioma growth, invasiveness and GSC propagation, by coordinately targeting *IGFBP2*, *EGFR*, *CDK6*, and *Bcl-xL* (Figure 5f). Further, because of existence of *MIR-491*deletion in a broad spectrum of cancer types, miR-491 holds promise as a broad therapeutic agent especially for cancers with chromosome 9p21.3 deletion.

MATERIALS AND METHODS

Many basic experimental procedures, including vector construction, luciferase reporter assay, real-time PCR, Western blot, MTT, colony-formation, soft-agar assay, neurosphere

formation, BrdU incorporation assay, cell apoptosis detection, and cell invasion assays are described in Supplemental Methods.

Tumor samples and RNA sequencing

Twenty human GBM samples were acquired from The University of Texas MD Anderson Cancer Center's Brain Tumor Center tissue bank under an institutional review board–approved protocol. GBM samples were pooled for SOLiD sequencing according to tumor type (four pools of five samples each). An additional pool of normal brain tissue samples (adult brain RNA sample pool, n = 23; Ambion, Carlsbad, CA) was used as reference. RNA extraction, library preparation, and transcriptome and small-RNA sequencing were performed as described previously[13]. Briefly, library preparation for both whole-transcriptome sequencing and small-RNA sequencing was performed according to the protocols of Applied Biosystems Incorporated (Carlsbad, CA). Sequencing runs were performed using Applied Biosystems' SOLiD System version 3.5 for both whole-transcriptome sequencing and small-RNA sequencing, which yielded over 610 million and 230 million 50-nt sequencing reads, respectively. Sequencing reads were aligned against transcript sequences from the National Center for Biotechnology Information reference sequence build version 38 using Bowtie version 0.12.5. Expression levels of miRNA and mRNA were determined by Reads, and Reads Per Kilobase of exon model per Million mapped reads (RPKM value), respectively.

Materials, cell culture, and transfection

U251 and T98G, obtained from American Type Culture Collection (Manassas, VA), were cultured in DMEM/F12 supplemented with 10% FBS. GSC cells were isolated from GBM tumor(s) that were removed from patients as previously described[25, 51, 52] and cultured in neural stem cell (NSC) medium [DMEM-F12 (1:1) supplemented with B27 (Invitrogen, Carlsbad, CA), 20 ng/ml bFGF, and 20 ng/ml EGF (Sigma, St. Louis, MO)]. The details are described in Supplemental Information. Primary murine astrocytes were isolated from *Ntv-a*;*Ink4a-Arf* null mice as described previously[26, 33] and maintained in DMEM with 10% FBS. All the cells were incubated at 37°C in an atmosphere containing 5% CO_2 and 20% O_2.

The miR-491-5p and miR-491-3p mimics, miR-491-5p hairpin inhibitor, and the corresponding negative controls were from Dharmacon (Chicago, IL). siRNAs targeting *IGFBP2* and *CDK6*, endoribonuclease prepared siRNA pools (esiRNAs) targeting *EGFR* and *Bcl-xL*, and scrambled negative siRNA control were from Sigma. miRNA mimic or siRNA was transected at a final concentration of 25 nM or 50 nM, using Lipofectamine RNAiMax (Invitrogen). pcDNA3.1(+)-Bcl-xL was generated by subcloning Bcl-xL fragment from pSFFV-neo Bcl-xL (Addgene plasmid 8749)[53] into the *Eco*RI site of pcDNA3.1(+). pCMV-CDK6 was from Addgene (plasmid 1868)[54]. pcDNA6-EGFR was provided by Dr. Mien-Chie Hung (MD Anderson Cancer Center). U251 cells stably expressing IGFBP2-EGFP and GFP were obtained by transfecting the cells with pEGFP-N3-IGFBP2 vector and pcDNA3-GFP vector (generated in our laboratory) using Lipofectamine 2000 (Invitrogen) respectively, subsequently selecting with 500 μg/mL G418 (Life Technologies, Grand Island, NY), and pooling the resultant single clones together. For GSC

rescue experiment, GSC 11 were transfected with *IGFBP2*-, *CKD6*-, *EGFR*-, or *Bcl-xL*–expressing constructs or empty pcDNA3.1(+) vector using the Amaxa Mouse Stem Cell Nucleofector Kit (Lonza, Allendale, NJ). Briefly, 10^6 GSCs were electroporated with 2 μg of indicated plasmid using the predefined Nucleofector program A-033 according to the manufacturer's instructions. Twenty-four hours later, cells were transfected with miR-491 mimics or control mimics using Lipofectamine RNAiMax (Invitrogen).

Tissue microarray construction, miRNA *in situ* hybridization, and immunohistochemical analysis

Tissue microarray (TMA) was constructed as described in Supplemental Information. miRNA *in situ* hybridization was performed as previously described[55]. Expression of hsa-miR-491-3p was detected by the double-DIG-labeled miRCURY LNA detection probe, hsa-miR-491-3p (38603-15; Exiqon, Woburn, MA). The details are described in Supplemental Information. Immunohistochemical staining was performed with a goat antibody against human IGFBP2 (1:300, SC-6001; Santa Cruz Biotechnology) and the HRP-DAB–based Cell and Tissue Staining Kit (R&D Systems, Minneapolis, MN). Intensity levels in tumor cells were manually quantified using a scoring system from 0 to 3 (0 = no signal, 1 = weak signal, 2 = intermediate signal, and 3 = strong signal). The staining for miR-491-3p was generally even throughout the tumor area. If the staining varied among regions within one sample, the average value of expression levels was marked as the expression level for that case. Altogether 146 cases (106 GBMs, 37 lower grade astrocytomas, and 3 oligoastrocytomas) were included in the final analysis. When the score for miR-491-3p was <2, miR-491-3p was considered to be expressed at a low level. TMA was examined and scored by two blinded neuropathologists.

Intracranial xenograft transplantation

Male athymic mice (nu/nu) were implanted in the brain with GSC 11 cells untreated, transfected with control mimics, or transfected with miR-491-5p and -3p together according to institution-approved protocols (10 mice per group). Briefly, mice were anesthetized with 0.25 ml of a cocktail of ketamine 10 mg/ml and xylazine 1 mg/ml, and cells were implanted by using cranial guide screws. A Hamilton syringe and microinfusion syringe pump (0.5 μl/min; Harvard Apparatus, Holliston, MA) were used to implant 1×10^5 cells into the brain of each mouse (10 mice simultaneously). Upon detection of an external tumor or obvious declining health, mice were killed by intracardiac perfusion of PBS and 4% paraformaldehyde according to IACUC guidelines. The mice survival was evaluated with Kaplan-Meier survival analysis.

Bioinformatics and statistical analysis

Gene expression data, chromosomal copy number variation data, miRNA expression data, and patient clinical data were obtained from the TCGA data portal (https://tcga-data.nci.nih.gov/tcga/findArchives.htm). For the purpose of integrative analysis, a core set of 388 samples was identified for which all the data types were available. Because of a limitation in technology, GBM miRNA expression data were available only for the major form of miR-491, miR-491-5p (Agilent 8x15K Human miRNA-specific microarray).

Pearson correlation analysis was performed using Matlab software. The two-sided Student *t*-test was used to assess the statistic difference unless otherwise specified. A *P*-value of less than 0.05 was considered statistically significant.

Supplementary Material

Refer to Web version on PubMed Central for supplementary material.

ACKNOWLEDGMENTS

We appreciate Xinna Zhang at MicroRNA Core Facility for help with miRNA hybridization experiments, Zhimin Lu at Department of Neuro-Oncology-Research for helpful comments, and Kathryn L. Hale at Department of Scientific Publications at MD Anderson Cancer Center for manuscript editing. This work was supported by grants from the National Institutes of Health (CA098503 to W.Z. and I.S., CA141432 and CA143835 to W.Z; .CA115729 and CA127001 to FFL), IVY, Elias and Broach Foundations, the Gene Pennebaker Brain Cancer Fund, and the Academy of Finland (grant 259038 to K.G.); Xia Li was supported by a fellowship from The Fourth Military Medical University (4138C4IA1Z). Lynette Moore was supported by a fellowship from the American Cancer Society.

References

1. Hanahan D, Weinberg RA. Hallmarks of cancer: the next generation. Cell. 2011; 144:646–674. [PubMed: 21376230]
2. Dong JT. Chromosomal deletions and tumor suppressor genes in prostate cancer. Cancer Metastasis Rev. 2001; 20:173–193. [PubMed: 12085961]
3. Testa JR, Liu Z, Feder M, Bell DW, Balsara B, Cheng JQ, et al. Advances in the analysis of chromosome alterations in human lung carcinomas. Cancer Genet Cytogenet. 1997; 95:20–32. [PubMed: 9140450]
4. Sato M, Takahashi K, Nagayama K, Arai Y, Ito N, Okada M, et al. Identification of chromosome arm 9p as the most frequent target of homozygous deletions in lung cancer. Genes Chromosomes Cancer. 2005; 44:405–414. [PubMed: 16114034]
5. Kohno T, Yokota J. Molecular processes of chromosome 9p21 deletions causing inactivation of the p16 tumor suppressor gene in human cancer: deduction from structural analysis of breakpoints for deletions. DNA Repair (Amst). 2006; 5:1273–1281. [PubMed: 16931177]
6. Sasaki S, Kitagawa Y, Sekido Y, Minna JD, Kuwano H, Yokota J, et al. Molecular processes of chromosome 9p21 deletions in human cancers. Oncogene. 2003; 22:3792–3798. [PubMed: 12802286]
7. Gursky S, Olopade OI, Rowley JD. Identification of a 1.2 Kb cDNA fragment from a region on 9p21 commonly deleted in multiple tumor types. Cancer Genet Cytogenet. 2001; 129:93–101. [PubMed: 11566337]
8. Bartel DP. MicroRNAs: target recognition and regulatory functions. Cell. 2009; 136:215–233. [PubMed: 19167326]
9. Calin GA, Croce CM. MicroRNA signatures in human cancers. Nat Rev Cancer. 2006; 6:857–866. [PubMed: 17060945]
10. Nakano H, Miyazawa T, Kinoshita K, Yamada Y, Yoshida T. Functional screening identifies a microRNA, miR-491 that induces apoptosis by targeting Bcl-X(L) in colorectal cancer cells. Int J Cancer. 2010; 127:1072–1080. [PubMed: 20039318]
11. Yan W, Zhang W, Sun L, Liu Y, You G, Wang Y, et al. Identification of MMP-9 specific microRNA expression profile as potential targets of anti-invasion therapy in glioblastoma multiforme. Brain Res. 2011; 1411:108–115. [PubMed: 21831363]
12. Parker BC, Annala MJ, Cogdell DE, Granberg KJ, Sun Y, Ji P, et al. The tumorigenic FGFR3-TACC3 gene fusion escapes miR-99a regulation in glioblastoma. J Clin Invest. 2013; 123:855–865. [PubMed: 23298836]

13. Moore LM, Kivinen V, Liu Y, Annala M, Cogdell D, Liu X, et al. Transcriptome and small RNA deep sequencing reveals deregulation of miRNA biogenesis in human glioma. J Pathol. 2013; 229:449–459. [PubMed: 23007860]
14. Fuxe J, Akusjarvi G, Goike HM, Roos G, Collins VP, Pettersson RF. Adenovirus-mediated overexpression of p15INK4B inhibits human glioma cell growth, induces replicative senescence, and inhibits telomerase activity similarly to p16INK4A. Cell Growth Differ. 2000; 11:373–384. [PubMed: 10939591]
15. Kim BN, Yamamoto H, Ikeda K, Damdinsuren B, Sugita Y, Ngan CY, et al. Methylation and expression of p16INK4 tumor suppressor gene in primary colorectal cancer tissues. Int J Oncol. 2005; 26:1217–1226. [PubMed: 15809712]
16. Zhang W, Fuller G. IGFBP2 as a brain tumor oncogene. Cancer Biol Ther. 2007; 6:995–996. [PubMed: 19358341]
17. Fukushima T, Tezuka T, Shimomura T, Nakano S, Kataoka H. Silencing of insulin-like growth factor-binding protein-2 in human glioblastoma cells reduces both invasiveness and expression of progression-associated gene CD24. J Biol Chem. 2007; 282:18634–18644. [PubMed: 17475624]
18. Lee EJ, Mircean C, Shmulevich I, Wang H, Liu J, Niemisto A, et al. Insulin-like growth factor binding protein 2 promotes ovarian cancer cell invasion. Mol Cancer. 2005; 4:7. [PubMed: 15686601]
19. Wang H, Wang H, Shen W, Huang H, Hu L, Ramdas L, et al. Insulin-like growth factor binding protein 2 enhances glioblastoma invasion by activating invasion-enhancing genes. Cancer Res. 2003; 63:4315–4321. [PubMed: 12907597]
20. Das S, Srikanth M, Kessler JA. Cancer stem cells and glioma. Nature clinical practice Neurology. 2008; 4:427–435.
21. Hsieh D, Hsieh A, Stea B, Ellsworth R. IGFBP2 promotes glioma tumor stem cell expansion and survival. Biochem Biophys Res Commun. 2010; 397:367–372. [PubMed: 20515648]
22. Lee J, Kotliarova S, Kotliarov Y, Li A, Su Q, Donin NM, et al. Tumor stem cells derived from glioblastomas cultured in bFGF and EGF more closely mirror the phenotype and genotype of primary tumors than do serum-cultured cell lines. Cancer Cell. 2006; 9:391–403. [PubMed: 16697959]
23. Griffero F, Daga A, Marubbi D, Capra MC, Melotti A, Pattarozzi A, et al. Different response of human glioma tumor-initiating cells to epidermal growth factor receptor kinase inhibitors. J Biol Chem. 2009; 284:7138–7148. [PubMed: 19147502]
24. Singh SK, Clarke ID, Terasaki M, Bonn VE, Hawkins C, Squire J, et al. Identification of a cancer stem cell in human brain tumors. Cancer Res. 2003; 63:5821–5828. [PubMed: 14522905]
25. Singh SK, Hawkins C, Clarke ID, Squire JA, Bayani J, Hide T, et al. Identification of human brain tumour initiating cells. Nature. 2004; 432:396–401. [PubMed: 15549107]
26. Dunlap SM, Celestino J, Wang H, Jiang R, Holland EC, Fuller GN, et al. Insulin-like growth factor binding protein 2 promotes glioma development and progression. Proc Natl Acad Sci U S A. 2007; 104:11736–11741. [PubMed: 17606927]
27. Jin X, Yin J, Kim SH, Sohn YW, Beck S, Lim YC, et al. EGFR-AKT-Smad signaling promotes formation of glioma stem-like cells and tumor angiogenesis by ID3-driven cytokine induction. Cancer Res. 2011; 71:7125–7134. [PubMed: 21975932]
28. Mirimanoff RO. High-grade gliomas: reality and hopes. Chin J Cancer. 2014; 33:1–3. [PubMed: 24384235]
29. Verhaak RG, Hoadley KA, Purdom E, Wang V, Qi Y, Wilkerson MD, et al. Integrated genomic analysis identifies clinically relevant subtypes of glioblastoma characterized by abnormalities in PDGFRA, IDH1, EGFR, and NF1. Cancer Cell. 2010; 17:98–110. [PubMed: 20129251]
30. Cancer Genome Atlas Research N. Comprehensive genomic characterization defines human glioblastoma genes and core pathways. Nature. 2008; 455:1061–1068. [PubMed: 18772890]
31. Rich JN, Reardon DA, Peery T, Dowell JM, Quinn JA, Penne KL, et al. Phase II trial of gefitinib in recurrent glioblastoma. J Clin Oncol. 2004; 22:133–142. [PubMed: 14638850]
32. Hegi ME, Diserens AC, Bady P, Kamoshima Y, Kouwenhoven MC, Delorenzi M, et al. Pathway analysis of glioblastoma tissue after preoperative treatment with the EGFR tyrosine kinase inhibitor gefitinib--a phase II trial. Mol Cancer Ther. 2011; 10:1102–1112. [PubMed: 21471286]

33. Moore LM, Holmes KM, Smith SM, Wu Y, Tchougounova E, Uhrbom L, et al. IGFBP2 is a candidate biomarker for Ink4a-Arf status and a therapeutic target for high-grade gliomas. Proc Natl Acad Sci U S A. 2009; 106:16675–16679. [PubMed: 19805356]
34. Wang GK, Hu L, Fuller GN, Zhang W. An interaction between insulin-like growth factor-binding protein 2 (IGFBP2) and integrin alpha5 is essential for IGFBP2-induced cell mobility. J Biol Chem. 2006; 281:14085–14091. [PubMed: 16569642]
35. Png KJ, Halberg N, Yoshida M, Tavazoie SF. A microRNA regulon that mediates endothelial recruitment and metastasis by cancer cells. Nature. 2012; 481:190–194. [PubMed: 22170610]
36. Feng J, Kim ST, Liu W, Kim JW, Zhang Z, Zhu Y, et al. An integrated analysis of germline and somatic, genetic and epigenetic alterations at 9p21.3 in glioblastoma. Cancer. 2012; 118:232–240. [PubMed: 21713760]
37. Holmes KM, Annala M, Chua CY, Dunlap SM, Liu Y, Hugen N, et al. Insulin-like growth factor-binding protein 2-driven glioma progression is prevented by blocking a clinically significant integrin, integrin-linked kinase, and NF-kappaB network. Proc Natl Acad Sci U S A. 2012; 109:3475–3480. [PubMed: 22345562]
38. Brockschmidt A, Trost D, Peterziel H, Zimmermann K, Ehrler M, Grassmann H, et al. KIAA1797/FOCAD encodes a novel focal adhesion protein with tumour suppressor function in gliomas. Brain : a journal of neurology. 2012; 135:1027–1041. [PubMed: 22427331]
39. Soeda A, Inagaki A, Oka N, Ikegame Y, Aoki H, Yoshimura S, et al. Epidermal growth factor plays a crucial role in mitogenic regulation of human brain tumor stem cells. J Biol Chem. 2008; 283:10958–10966. [PubMed: 18292095]
40. Ayuso-Sacido A, Moliterno JA, Kratovac S, Kapoor GS, O'Rourke DM, Holland EC, et al. Activated EGFR signaling increases proliferation, survival, and migration and blocks neuronal differentiation in post-natal neural stem cells. J Neurooncol. 2010; 97:323–337. [PubMed: 19855928]
41. Beukelaers P, Vandenbosch R, Caron N, Nguyen L, Belachew S, Moonen G, et al. Cdk6-dependent regulation of G(1) length controls adult neurogenesis. Stem Cells. 2011; 29:713–724. [PubMed: 21319271]
42. Zhou Z, Sun L, Wang Y, Wu Z, Geng J, Miu W, et al. Bone morphogenetic protein 4 inhibits cell proliferation and induces apoptosis in glioma stem cells. Cancer biotherapy & radiopharmaceuticals. 2011; 26:77–83. [PubMed: 21355779]
43. Silber J, Lim DA, Petritsch C, Persson AI, Maunakea AK, Yu M, et al. miR-124 and miR-137 inhibit proliferation of glioblastoma multiforme cells and induce differentiation of brain tumor stem cells. BMC Med. 2008; 6:14. [PubMed: 18577219]
44. Guessous F, Zhang Y, Kofman A, Catania A, Li Y, Schiff D, et al. microRNA-34a is tumor suppressive in brain tumors and glioma stem cells. Cell Cycle. 2010; 9:1031–1036. [PubMed: 20190569]
45. Papagiannakopoulos T, Friedmann-Morvinski D, Neveu P, Dugas JC, Gill RM, Huillard E, et al. Pro-neural miR-128 is a glioma tumor suppressor that targets mitogenic kinases. Oncogene. 2012; 31:1884–1895. [PubMed: 21874051]
46. Kefas B, Godlewski J, Comeau L, Li Y, Abounader R, Hawkinson M, et al. microRNA-7 inhibits the epidermal growth factor receptor and the Akt pathway and is down-regulated in glioblastoma. Cancer Res. 2008; 68:3566–3572. [PubMed: 18483236]
47. Hai C, Jin YM, Jin WB, Han ZZ, Cui MN, Piao XZ, et al. Application of mesenchymal stem cells as a vehicle to deliver replication-competent adenovirus for treating malignant glioma. Chin J Cancer. 2012; 31:233–240. [PubMed: 22429494]
48. Bexell D, Svensson A, Bengzon J. Stem cell-based therapy for malignant glioma. Cancer Treat Rev. 2013; 39:358–365. [PubMed: 22795538]
49. Yin J, Kim JK, Moon JH, Beck S, Piao D, Jin X, et al. hMSC-mediated concurrent delivery of endostatin and carboxylesterase to mouse xenografts suppresses glioma initiation and recurrence. Mol Ther. 2011; 19:1161–1169. [PubMed: 21386822]
50. Hwang do W, Son S, Jang J, Youn H, Lee S, Lee D, et al. A brain-targeted rabies virus glycoprotein-disulfide linked PEI nanocarrier for delivery of neurogenic microRNA. Biomaterials. 2011; 32:4968–4975. [PubMed: 21489620]

51. Jiang H, Gomez-Manzano C, Aoki H, Alonso MM, Kondo S, McCormick F, et al. Examination of the therapeutic potential of Delta-24-RGD in brain tumor stem cells: role of autophagic cell death. J Natl Cancer Inst. 2007; 99:1410–1414. [PubMed: 17848677]

52. He H, Nilsson CL, Emmett MR, Marshall AG, Kroes RA, Moskal JR, et al. Glycomic and transcriptomic response of GSC11 glioblastoma stem cells to STAT3 phosphorylation inhibition and serum-induced differentiation. J Proteome Res. 2010; 9:2098–2108. [PubMed: 20199106]

53. Chao DT, Linette GP, Boise LH, White LS, Thompson CB, Korsmeyer SJ. Bcl-XL and Bcl-2 repress a common pathway of cell death. J Exp Med. 1995; 182:821–828. [PubMed: 7650488]

54. van den Heuvel S, Harlow E. Distinct roles for cyclin-dependent kinases in cell cycle control. Science. 1993; 262:2050–2054. [PubMed: 8266103]

55. Sempere LF, Christensen M, Silahtaroglu A, Bak M, Heath CV, Schwartz G, et al. Altered MicroRNA expression confined to specific epithelial cell subpopulations in breast cancer. Cancer Res. 2007; 67:11612–11620. [PubMed: 18089790]

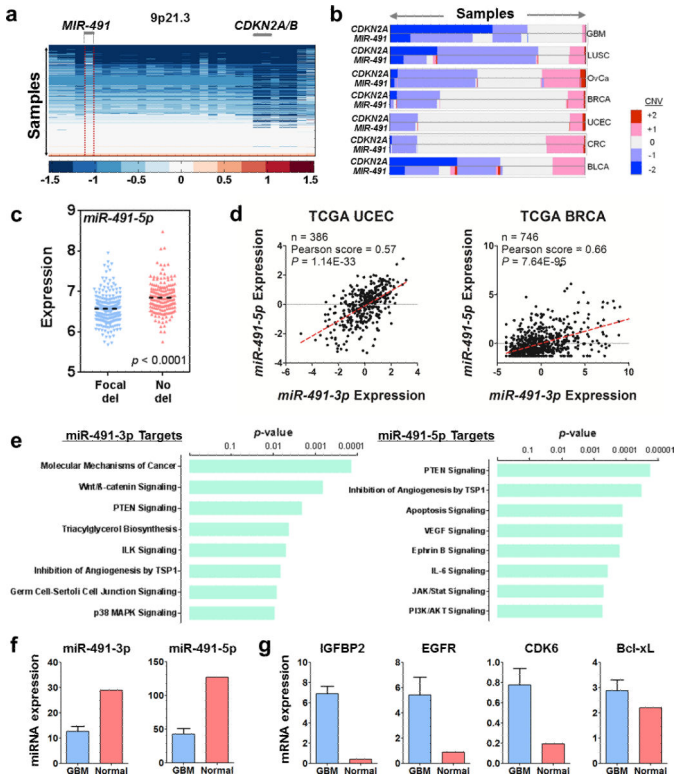

Figure 1. miR-491-5p and -3p are downregulated in GBM and their expression inversely correlated with that of *IGFBP2, EGFR, CDK6,* and *Bcl-xL*

(a) Deletion of 9p21.3 is frequent in TCGA GBM data. Segmented DNA copy-number data from SNP arrays are shown. Each row represents a patient; deleted regions are shown in blue. **(b)** Chromosomal copy number variations (CNV) of both *CDKN2A* and *MIR-491* in different cancer types from TCGA. GBM, glioblastoma multiforme; LUSC, Lung squamous cell carcinoma; OvCa, Ovarian serous cystadenocarcinoma; BRCA, Breast invasive carcinoma; UCEC, Uterine corpus endometrioid carcinoma; CRC, Colon and rectum adenocarcinoma; BLCA, Bladder urothelial carcinoma. **(c)** Genomic loss (del) leads to a significant decrease in miR-491-5p expression ($p < 0.0001$). **(d)** The expression of miR-491-3p and miR-491-5p measured via miRNA sequencing exhibited a similar pattern in the TCGA endometrial (UCEC) and breast (BRCA) cancer data sets. **(e)** Significantly enriched pathways in the targets of miR-491-3p and miR-491-5p are shown. **(f)** Expression of miR-491-5p and miR-491-3p is lower in GBMs than in normal brain controls. Expression levels of miR-491-5p and miR-491-3p were determined by Reads from small-RNA deep sequencing of pooled GBM and pooled normal brain tissue samples. **(g)** mRNA levels of *IGFBP2*, *CDK6*, *EGFR*, and *Bcl-xL* are higher in GBMs than in pooled normal brain controls. Expression levels of *IGFBP2*, *CDK6*, *EGFR*, and *Bcl-xL* were determined in terms of Reads Per Kilobase of exon model per Million mapped reads (RPKM values) from the whole-transcriptome deep-sequencing of GBMs and normal brain tissues.

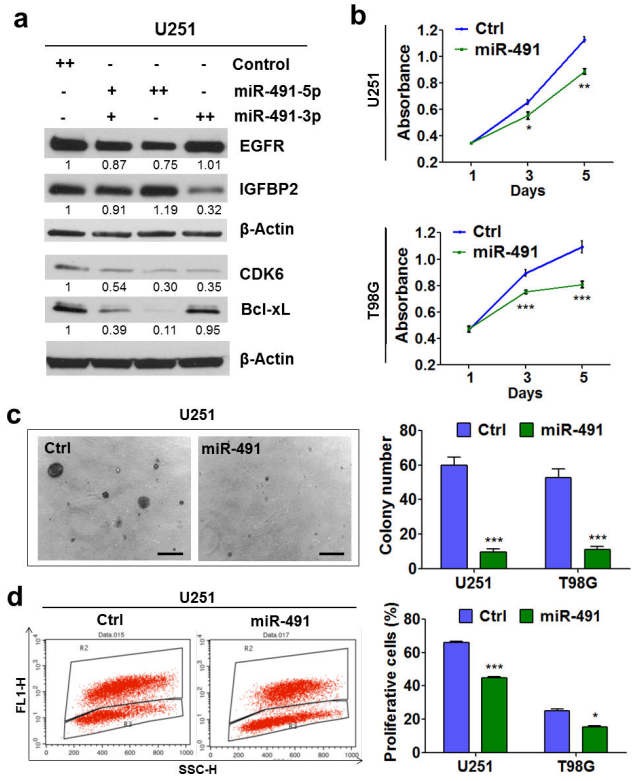

Figure 2. miR-491-5p and/or miR-491-3p directly target *IGFBP2, CDK6, EGFR,* and *Bcl-xL* and regulate GBM cell proliferation

(a) miR-491-5p/miR-491-3p regulates IGFBP2, CDK6, EGFR, and Bcl-xL expression at the protein level. Beta-actin was used as a protein loading control. Each band's intensity was quantified by using Image J, and the relative values (beta-actin as internal control) were shown below the bands. +: 25nM; ++: 50 nM. **(b)** miR-491 inhibits glioma cell growth. Cell viability of U251 and T98G cells transfected with both miR-491-5p and miR-491-3p mimics or with control mimics was monitored by MTT assay (n = 6). **(c)** miR-491 inhibits soft agar colonization by glioma cell lines. Upon transfection, cells were seeded into the soft agar and the numbers of colonies were determined four weeks later (n = 3); representative colony morphologies of U251 are shown (n = 3). Bar: 200 μm. **(d)** miR-491 inhibits glioma cell proliferation. BrdU incorporation assay (n=3) was done seventy-two hours after transfection. Data are presented as mean ± SD (*, $P<0.05$; **, $P<0.01$; ***, $P<0.001$, Student *t* test).

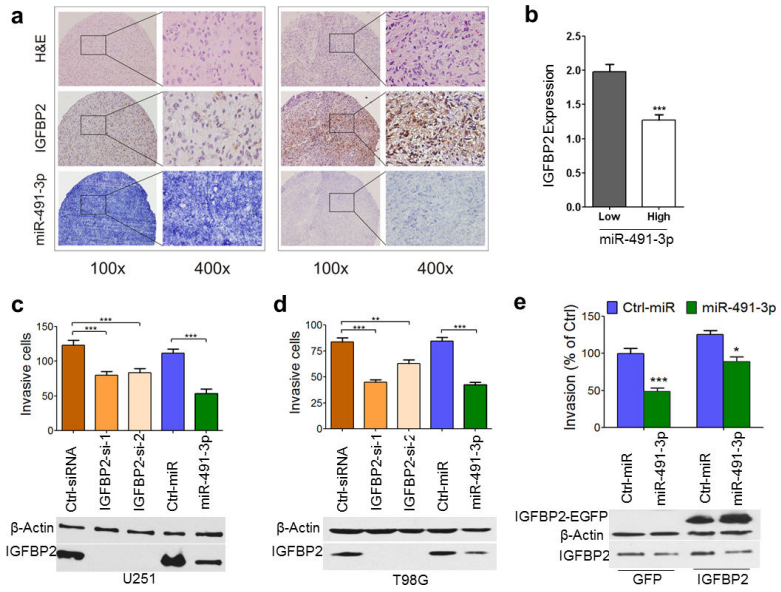

Figure 3. miR-491-3p inhibits glioma cell invasion

(a, b) Expression of miR-491-3p inversely correlates with IGFBP2 protein level. Transcript stability in each sample was verified by using U6 as an internal control. Representative images of *in situ* hybridization staining for miR-491-3p and immunohistochemical staining for IGFBP2 are shown in (a). Data in panel b is presented as mean ± SEM (***, P=0.0002, Mann Whitney test). **(c, d)** miR-491-3p inhibits invasion of U251 (c) and T98G (d) cells. Invading cells were counted in ten randomly chosen fields under the microscope (n = 3). **(e)** IGFBP2 partly overcomes the inhibitory effect of miR-491-3p on cell invasion in U251 cells. Levels of exogenous (IGFBP2-EGFP) and endogenous IGFBP2 were determined by Western blot (lower panel). Beta-actin was used as a protein loading control. GFP or IGFBP2 represent U251 cells stably expressing either GFP or IGFBP2-EGFP, respectively. Cell invasion was calculated as the number of invasive cells divided by the number of invasive U251-GFP cells that were transfected with control mimics (upper panel) (n = 3). In c, d and e, data are presented as mean ± SD (*, P<0.05; **, P<0.01; ***, P<0.001, Student t test).

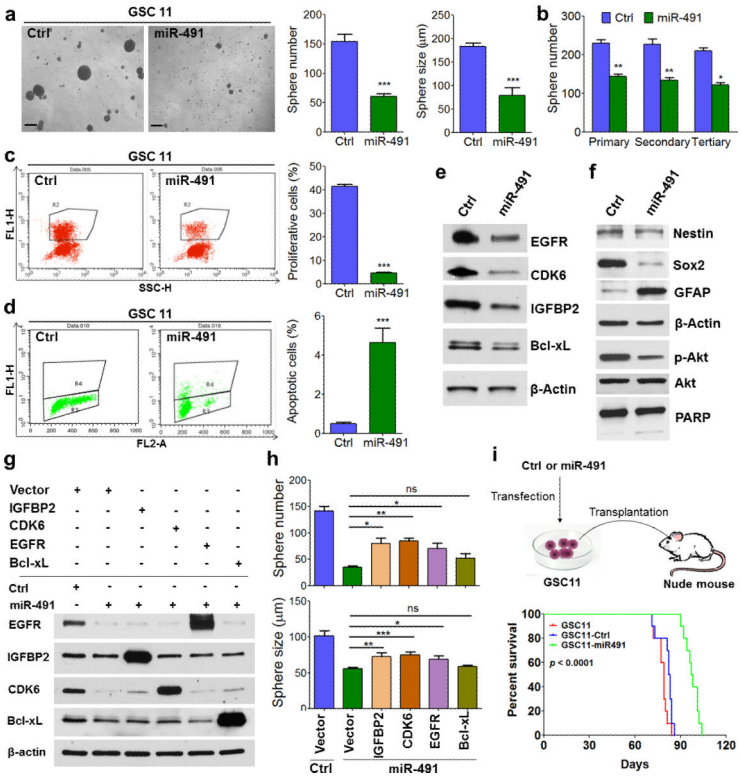

Figure 4. miR-491 inhibits GSC propagation *in vitro and in vivo*

(a) miR-491 inhibits neurosphere formation of GSC 11. Patient-derived GSC 11 upon transfection were cultured in NSC medium, and the number of spheres and their diameters were determined 7 days later; representative sphere morphologies are shown (n = 3). Bar: 100 μm. **(b)** miR-491 inhibits self-renewal of GSC 11. Transfected GSC11 were cultured in NSC medium to form neurospheres and serially passaged every 7 days. The number of primary, secondary, and tertiary neurospheres were determined respectively (n = 3). **(c)** miR-491 inhibits GSC proliferation.GSC11 cells were subjected to BrdU incorporation assay seventy-two hours after transfection. **(d)** miR-491 induces GSC apoptosis. Apoptotic cells were identified by APO-BrdU kit seventy-two hours after transfection; PARP cleavage was determined by Western blot (in f). **(e, f)** miR-491 overexpression leads to reduction of EGFR, CDK6, IGFBP2, and Bcl-xL (e), reduction of p-Akt, Nestin, and Sox2 (f), as well as upregulation of GFAP in GSC11 cells (f). **(g, h)** IGFBP2, CDK6, or EGFR overexpression partially overcomes the inhibitory effect of miR-491 on neurosphere formation. GSC 11 cells were transfected as described in Methods. IGFBP2, CDK6, EGFR and Bcl-xL levels were analyzed by Western blot 48 hours after transfection (g) and the number of spheres and their diameters were determined 7 days later (h) (n = 3). In a-d and h, data are presented as mean ± SD (*, $P<0.05$; **, $P<0.01$; ***, $P<0.001$, Student t test). **(i)** miR-491 prolongs the survival of the mice orthotopically transplanted with GSC11 cells. Kaplan-Meier survival curves were shown for the nude mice transplanted with GSC 11 cells that were either untreated, transfected with control mimics, or transfected with both miR-491-5p and miR-491-3p mimics (n = 10 per group; P<0.0001, log-rank test).

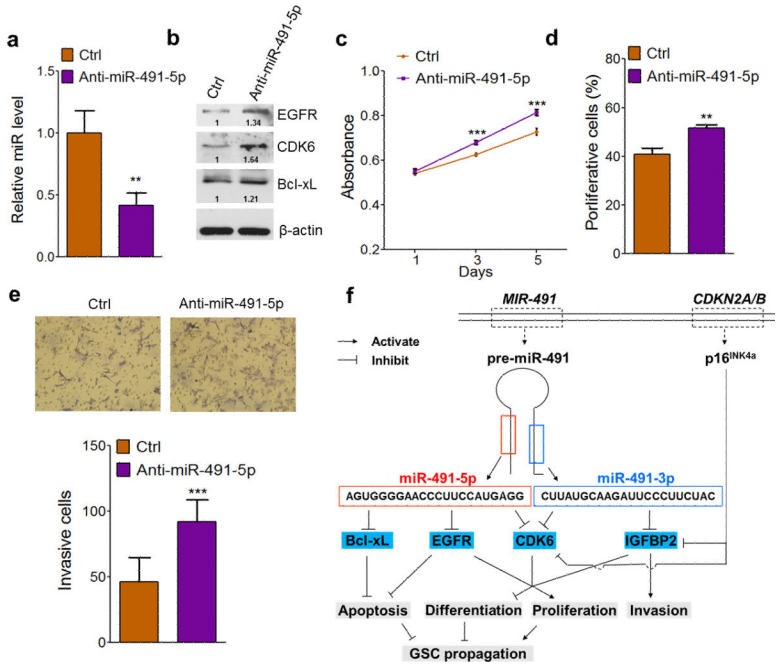

Figure 5. Knockdown of miR-491-5p exacerbates malignancy of *Ink4a-Arf*-null mouse glial progenitor cells

(a) Knockdown efficiency of anti-miR-491-5p (hairpin inhibitor). Forty-eight hours after transfection with anti-miR-491-5p, miR-491-5p levels were assessed by quantitative PCR. **(b)** Anti-miR-491-5p upregulates mouse CDK6, EGFR, and Bcl-xL expression. Beta-actin was used as a protein loading control. Number below each blot indicates relative band intensity (quantified by Image J). **(c)** Anti-miR-491-5p promotes the growth of *Ink4a-Arf*-null mouse glial progenitor cells. Cell viability was monitored by MTT assay (n = 6). **(d)** Anti-miR-491 enhances cell proliferation. Proliferating cells were analyzed with BrdU incorporation assay seventy-two hours after transfection. **(e)** Anti-miR-491 promotes cell invasion. Invading cells were counted in ten randomly chosen fields under the microscope, with the representative photographs taken at 100 × magnification (n = 3). Data are presented as mean ± SD (*, $P<0.05$; **, $P<0.01$; ***, $P<0.001$, Student *t* test). **(f)** The proposed model for the function of miR-491-5p and -3p and the cooperation between *CDKN2A* and *MIR-491* genomic loss in GBM.